Viscous potential flow analysis of radial fingering in a Hele-Shaw cell

Cite as: Phys. Fluids **21**, 074106 (2009); https://doi.org/10.1063/1.3184574
Submitted: 15 March 2009 • Accepted: 17 June 2009 • Published Online: 22 July 2009

Hyungjun Kim, Toshio Funada, Daniel D. Joseph, et al.

Viscous potential flow analysis of radial fingering in a Hele-Shaw cell

Hyungjun Kim,[1,a)] Toshio Funada,[2,a)] Daniel D. Joseph,[3,a)] and G. M. Homsy[4,b)]
[1]*Department of Mechanical Engineering, KAIST, 335 Gwahangno, Yuseong-gu, Daejeon 305-701, South Korea*
[2]*Department of Digital Engineering, Numazu National College of Technology, Numazu, Shizuoka 410-8501, Japan*
[3]*Department of Aerospace Engineering and Mechanics, University of Minnesota, Minneapolis, Minnesota 55455, USA and Department of Mechanical and Aerospace Engineering, University of California, Irvine, California 92617, USA*
[4]*Department of Mechanical Engineering, University of California at Santa Barbara, Santa Barbara, California 93106, USA*

(Received 15 March 2009; accepted 17 June 2009; published online 22 July 2009; publisher error corrected 24 July 2009)

The problem of radial fingering in two phase gas/liquid flow in a Hele-Shaw cell under injection of gas is studied here. The fingers arise as an instability of a time-dependent flow. The instability is analyzed as a viscous potential flow, in which potential flow analysis of Paterson [L. Paterson, J. Fluid Mech. **113**, 513 (1981)] and others is augmented to account for the effects of viscosity on the normal stress at the gas/liquid interface. The addition of these new effects brings our theory into a much better agreement with experiments of Maxworthy [T. Maxworthy, Phys. Rev. A **39**, 5863 (1989)] than other theories. © *2009 American Institute of Physics*. [DOI: 10.1063/1.3184574]

I. INTRODUCTION

A Hele-Shaw cell is a device whose essential features are two closely spaced parallel plates containing a thin layer of viscous fluid. The equations governing the flow of the viscous fluid in the gap are similar to those governing the flow in a saturated porous medium, but important differences arise in the case of the equations that must be satisfied at a free gas/liquid surface and, of course, in the way the nonlinear terms appear in the two problems. This paper focuses on effects of the viscous normal stress which are neglected in all works on Hele-Shaw flow in the radial injection of gas into liquid.[1–10] The only mention of the viscous normal stress that we could find in the literature is in the paper by Pitts,[11] p. 60 where he notes that "If we ignore the contribution to the normal stress arising from the viscosity and velocity gradient (this can be shown to be small compared to the curvature in the x, y plane) we obtain for the pressure p_0 at the origin…." We do not wish to evaluate this statement for the Saffman–Taylor experiment studied by Pitts,[11] but it is not correct for the case of radial fingering studied by Paterson,[1] as we shall show here.

Under constant injection of gas, the volume of gas in the cell must continuously increase at a constant rate. In the basic state, the volume of gas increases in a circular disk which at some radius $R(t)$ nucleates into fingers. After this, the increasing gas volume is achieved by the growth of fingers.

II. GOVERNING EQUATIONS FOR INJECTION

From Paterson,[1] the definition of the potential is $\phi_j = M_j p_j$, $\boldsymbol{v}_j = -M_j \nabla p_j = -\nabla \phi_j$, for $j=1,2$ with the mobility M_j. In a basic state, fluid "1" is inside $(0 \le r < R)$ and fluid "2" is outside $(R < r < \infty)$, where $R \equiv R(t)$. The volume flow $\dot{V}$ of fluid 1 is expressed as $\dot{V} = Qb$ where Q is the circular area velocity and b the width of two plates. Integration of $\dot{V}$ with respect to time t gives

$$V - V_0 = \pi R^2 b - \pi R_0^2 b = Qbt \rightarrow R = \sqrt{\frac{Q}{\pi} t + R_0^2}, \tag{1}$$

where R_0 is the initial radius of the interface. For injection with $Q>0$, R increases from R_0. For withdrawal with $Q<0$, R decreases from R_0 and is terminated at $t=t_e$ for which $Qt_e + \pi R_0^2 = 0$. Withdrawal is easily obtained from injection and will not be discussed further.

The velocity potential ϕ_j for $j=1,2$ satisfies the equation of continuity

$$\frac{\partial^2 \phi_j}{\partial r^2} + \frac{1}{r}\frac{\partial \phi_j}{\partial r} + \frac{1}{r^2}\frac{\partial^2 \phi_j}{\partial \theta^2} = 0, \tag{2}$$

and pressure is given by $p_j = \phi_j / M_j$. The kinematic condition and the normal stress balance are required. The kinematic condition at the interface $r = R + a(t,\theta)$ is expressed as

$$\frac{\partial (r - R - a)}{\partial t} - \frac{\partial \phi_j}{\partial r}\frac{\partial (r - R - a)}{\partial r} - \left(\frac{1}{r}\frac{\partial \phi_j}{\partial \theta}\right)\frac{1}{r}\frac{\partial (r - R - a)}{\partial \theta} = 0. \tag{3}$$

The normal stress balance at $r = R(t) + a(t,\theta)$ is expressed as

[a)]Authors of article are Hyungjun Kim, Toshio Funada, and Daniel D. Joseph.
[b)]Author of appendix is G. M. Homsy.

$$p_1 + 2\mu_1\left[n_r^2\frac{\partial^2\phi_1}{\partial r^2} + n_r n_\theta\left(\frac{1}{r}\frac{\partial^2\phi_1}{\partial r\,\partial\theta} - \frac{1}{r^2}\frac{\partial\phi_1}{\partial\theta}\right) + n_\theta^2\left(\frac{1}{r^2}\frac{\partial^2\phi_1}{\partial\theta^2} + \frac{1}{r}\frac{\partial\phi_1}{\partial r}\right)\right] - p_2 - 2\mu_2\left[n_r^2\frac{\partial^2\phi_2}{\partial r^2} + n_r n_\theta\left(\frac{1}{r}\frac{\partial^2\phi_2}{\partial r\,\partial\theta} - \frac{1}{r^2}\frac{\partial\phi_2}{\partial\theta}\right) + n_\theta^2\left(\frac{1}{r^2}\frac{\partial^2\phi_2}{\partial\theta^2} + \frac{1}{r}\frac{\partial\phi_2}{\partial r}\right)\right] = \sigma\left(\frac{2}{b} + \nabla\cdot\boldsymbol{n}\right), \tag{4}$$

where σ is the surface tension coefficient and the unit normal vector is $\boldsymbol{n}$; the normal viscous stress is taken into account in the normal stress balance.

A. Basic flow

Let the velocity potential $\phi_j = \phi_{0j} + \phi_{1j}$ where ϕ_{0j} for basic and ϕ_{1j} for perturbed flow of gas/liquid interface. For basic flow, the interface is given by $r = R(t)$, where the mean radius $R(t)$ satisfies $\pi R(t)^2 = \pi R_0^2 + Qt$. The velocity potential satisfies Laplace's equation and is given by

$$\phi_{01}(r,t) = -\frac{Q}{2\pi}[\ln(r) - \ln(R(t))] - \frac{Q}{2\pi}\frac{M_1}{M_2} + c(t), \tag{5}$$

$$\phi_{02}(r,t) = -\frac{Q}{2\pi}[\ln(r) - \ln(R(t))] - \frac{Q}{2\pi}. \tag{6}$$

The kinematic condition at the interface is given by

$$\frac{\partial R}{\partial t} = -\left(\frac{\partial\phi_{01}}{\partial r}\right)_{r=R}, \quad \frac{\partial R}{\partial t} = -\left(\frac{\partial\phi_{02}}{\partial r}\right)_{r=R}. \tag{7}$$

Then the pressure is given by $p_{0j}(r,t) = \phi_{0j}(r,t)/M_j$ where $j = 1,2$. And, the normal stress balance follows is given by

$$p_{01}(R,t) + 2\mu_1\left(\frac{\partial^2\phi_{01}(r,t)}{\partial r^2}\right)_{r=R} - p_{02}(R,t) - 2\mu_2\left(\frac{\partial^2\phi_{02}(r,t)}{\partial r^2}\right)_{r=R} = \sigma\left(\frac{2}{b} + \frac{1}{R(t)}\right), \tag{8}$$

which provides $c(t)$:

$$\frac{c(t)}{M_1} - \sigma\left(\frac{2}{b} + \frac{1}{R(t)}\right) + \frac{Q}{\pi R(t)^2}(\mu_1 - \mu_2) = 0. \tag{9}$$

The first part is the pressure difference, the second the surface tension, and the third is due to viscous normal stress. The effect of the viscous normal stress on the evaluation of the forces acting on the perturbed interface was neglected by all previous authors.

B. Perturbed flow

The perturbed interface is given by $r = R(t) + a(t,\theta)$, for which the interface displacement with azimuthal mode n may be expressed as $a(t,\theta) = A_0 f(t)\exp(in\theta) + \text{c.c.}$, whence the volume is given, for the small disturbance, by

$$V = \int_0^{2\pi}\frac{b}{2}[R(t) + a(t,\theta)]^2 d\theta = \int_0^{2\pi}\frac{b}{2}[R(t)^2 + 2R(t)a(t,\theta)]d\theta = \pi R(t)^2 b. \tag{10}$$

The velocity potentials are given by

$$\phi_{1j}(r,t,\theta) = (-1)^j A_0 e^{in\theta}\left(\frac{r}{R(t)}\right)^{(-1)^{j-1}n} \times\left[\frac{Qf(t)}{2n\pi R(t)} + \frac{R}{n}f'(t)\right] + \text{c.c.}, \quad j = 1,2, \tag{11}$$

which satisfy the kinematic condition at the interface $r = R(t) + a(t,\theta)$

$$\frac{\partial a}{\partial t} = -\left(\frac{\partial^2\phi_{0j}}{\partial r^2}\right)_{r=R} a - \left(\frac{\partial\phi_{1j}}{\partial r}\right)_{r=R}, \quad j = 1,2, \tag{12}$$

and the pressures are expressed as $p_{1j}(r,t,\theta) = \phi_{1j}(r,t,\theta)/M_j$.

The normal stress balance for the perturbed field at $r = R + a(t,\theta)$ is given by

$$p_{01} + 2\mu_1\frac{\partial^2\phi_{01}}{\partial r^2} - \left(p_{02} + 2\mu_2\frac{\partial^2\phi_{02}}{\partial r^2}\right) + p_{11} + 2\mu_1\frac{\partial^2\phi_{11}}{\partial r^2} - \left(p_{12} + 2\mu_2\frac{\partial^2\phi_{12}}{\partial r^2}\right) = \left[p_{01} + 2\mu_1\frac{\partial^2\phi_{01}}{\partial r^2} - \left(p_{02} + 2\mu_2\frac{\partial^2\phi_{02}}{\partial r^2}\right)\right]_{r=R} + \left\{\frac{\partial}{\partial r}\left[p_{01} + 2\mu_1\frac{\partial^2\phi_{01}}{\partial r^2} - \left(p_{02} + 2\mu_2\frac{\partial^2\phi_{02}}{\partial r^2}\right)\right]\right\}_{r=R} a + \left[p_{11} + 2\mu_1\frac{\partial^2\phi_{11}}{\partial r^2} - \left(p_{12} + 2\mu_2\frac{\partial^2\phi_{12}}{\partial r^2}\right)\right]_{r=R} = \sigma\left[\frac{2}{b} + \frac{1}{R(t)} - \frac{a}{R(t)^2} - \frac{1}{R(t)^2}\frac{\partial^2 a}{\partial\theta^2}\right], \tag{13}$$

which is then arranged, after using Eq. (8), as

$$\left\{\frac{\partial}{\partial r}\left[p_{01}+2\mu_1\frac{\partial^2\phi_{01}}{\partial r^2}-\left(p_{02}+2\mu_2\frac{\partial^2\phi_{02}}{\partial r^2}\right)\right]\right\}_{r=R}a + \left[p_{11}+2\mu_1\frac{\partial^2\phi_{11}}{\partial r^2}-\left(p_{12}+2\mu_2\frac{\partial^2\phi_{12}}{\partial r^2}\right)\right]_{r=R} + \sigma\left(\frac{a}{R(t)^2}+\frac{1}{R(t)^2}\frac{\partial^2 a}{\partial\theta^2}\right)=0. \tag{14}$$

The normal stress difference of the basic field in Eq. (14) is expanded as

$$\left\{\frac{\partial}{\partial r}\left[p_{01}+2\mu_1\frac{\partial^2\phi_{01}}{\partial r^2}-\left(p_{02}+2\mu_2\frac{\partial^2\phi_{02}}{\partial r^2}\right)\right]\right\}_{r=R}a = -\frac{Qf(t)}{2\pi R(t)}\left[\frac{4}{R(t)^2}(\mu_1-\mu_2)+\frac{1}{M_1}-\frac{1}{M_2}\right]A_0e^{in\theta}+\text{c.c.} \tag{15}$$

Thus, the normal stress balance for the perturbed field Eq. (14) is given by

$$\left[p_{11}+2\mu_1\frac{\partial^2\phi_{11}}{\partial r^2}-\left(p_{12}+2\mu_2\frac{\partial^2\phi_{12}}{\partial r^2}\right)\right]_{r=R} + \sigma\left[\frac{a}{R(t)^2}+\frac{1}{R(t)^2}\frac{\partial^2 a}{\partial\theta^2}\right] = \left\{-\frac{(n^2-1)\sigma}{R(t)^2}f(t)-Q\left[\frac{(n-1)\mu_1+(n+1)\mu_2}{\pi R(t)^3}f(t) + \frac{M_1+M_2}{2M_1M_2n\pi R(t)}f(t)\right]-\left[\frac{(M_1+M_2)R(t)}{M_1M_2n} + \frac{2(n-1)\mu_1+2(n+1)\mu_2}{R(t)}\right]f'(t)\right\}A_0e^{in\theta}+\text{c.c.} \tag{16}$$

With $\mu_1=b^2/(12M_1)$ and $\mu_2=b^2/(12M_2)$, Eq. (13) is given as

$$-\frac{(n^2-1)\sigma}{R(t)^2}-\frac{b^2[M_1(n-1)+M_2(n+1)]}{12M_1M_2\pi R(t)^3}Q + \frac{M_1(n-1)-M_2(n+1)}{2M_1M_2n\pi R(t)}Q = \left\{\frac{b^2[M_2(n-1)+M_1(n+1)]}{6M_1M_2R(t)}+\frac{(M_1+M_2)R(t)}{M_1M_2n}\right\}\frac{f'(t)}{f(t)}. \tag{17}$$

If $[M_1(n-1)-M_2(n+1)]$ is positive for $n>1$, it causes instability, but the viscous term due to viscous potential flow (VPF) and the surface tension act as stabilizing. Also, Eq. (17) with $b^2=0$ goes to Eq. (10) of Paterson.[1]

To investigate the effects of VPF terms proportional to b^2, consider the case $\sigma=0$ when the finger number $n\gg1$. In this case

$$\frac{f'(t)}{f(t)}=-\frac{b^2n^2(M_1+M_2)+6n(M_2-M_1)R(t)^2}{b^2n^2(M_2+M_1)+6(M_1+M_2)R(t)^2}\times\frac{Q}{2\pi R(t)^2}. \tag{18}$$

When $n\to\infty$,

$$\frac{f'(t)}{f(t)}\to-\frac{Q}{2\pi R(t)^2}, \tag{19}$$

and the VPF terms are stabilizing. On the other hand, when $b^2=0$

$$\frac{f'(t)}{f(t)}=-\frac{n(M_2-M_1)Q}{(M_2+M_1)2\pi R(t)^2}>0, \tag{20}$$

so that large finger numbers are unstable and since $f'/f\propto n$, they are *Hadamard unstable*; large finger numbers grow with n without limit for any time no matter how small, as $n\to\infty$.

III. DISPERSION RELATION IN DIMENSIONLESS FORM

The scales for time and length are put as

$$(t,R)=(T\tau,b\xi),\quad \text{with } T=\frac{2b^2\pi}{Q}. \tag{21}$$

The dimensionless parameters are defined as

$$m=\frac{M_2}{M_1}=\frac{\mu_1}{\mu_2},\quad N_{\text{Ca}}=\frac{\dot{R}\mu_2}{\sigma}, \tag{22}$$

where $\dot{R}$ is the velocity of the interface. Also for the capillary number N_{Ca}, this can be divided by two dimensionless parameters as

$$N_{\text{Ca}}=\frac{1}{12P\xi},\quad \text{with } P=\frac{\pi b\sigma}{6Q\mu_2}, \tag{23}$$

and P is a more appropriate parameter than the capillary number N_{Ca} because it depends only on prescribed parameters and not on the solution.

For injection, the conservation of the volume flow is $\xi^2=\xi_0^2+2\tau$ and the dispersion relation is given by

$$-\frac{(n^2-1)}{\xi^2}P-\frac{m(n+1)+n-1}{6\xi^3}-\frac{m(n+1)-n+1}{n\xi} = \left[\frac{m(n-1)+n+1}{6\xi}+\frac{(m+1)\xi}{n}\right]\frac{f'(\tau)}{f(\tau)}. \tag{24}$$

We may define the growth rate $\alpha\equiv f'(\tau)/f(\tau)$ as a function of τ and β is the left-hand side of Eq. (24). The cutoff is given by $\beta=0$ in place of $\alpha=0$, since the coefficient of $f'(\tau)/f(\tau)$ is positive for $n>1$.

A. Critical condition

From Eq. (24), we have β at $n=1$ and 2 as

$$n=1\begin{cases}\beta_1=-\dfrac{m}{3\xi^3}-\dfrac{2m}{\xi}<0,\\ \beta_{1P}=-\dfrac{2m}{\xi}<0,\end{cases} \tag{25}$$

$$n=2\begin{cases}\beta_2=-\dfrac{3}{\xi^2}P-\dfrac{3m+1}{6\xi^3}-\dfrac{3m-1}{2\xi},\\ \beta_{2P}=-\dfrac{3}{\xi^2}P-\dfrac{3m-1}{2\xi}.\end{cases} \tag{26}$$

It is noted that $\beta_1<0$ gives $\alpha_1<0$. Paterson's case is given by β_{1P} and β_{2P}. The mode $n=1$ is marginally stable and leads to a shift of the center of the circular interface and stable. Instabilities may arise for $n>1$. It is expected that instability first arises at $n=2$, for which $\beta_2>0$ gives $\alpha_2>0$.

When $m=0$, we have

$$\beta_{20}=\frac{1}{2\xi^3}\left(\xi^2-6P\xi-\frac{1}{3}\right),$$

$$\beta_{20P}=\frac{1}{2\xi^3}(\xi^2-6P\xi). \tag{27}$$

The equation $\beta_{20}=0$ gives one solution

$$\xi=3P\pm\sqrt{9P^2+\frac{1}{3}}\rightarrow\xi=3P+\sqrt{9P^2+\frac{1}{3}}\equiv\xi_c. \tag{28}$$

The equation $\beta_{20P}=0$ for Paterson[1] case gives one solution $\xi=6P\equiv\xi_c$. For given values of P, a necessary condition for instability is denoted as $\xi>\xi_c$. For given values of ξ, a necessary condition for instability is denoted as $P<\xi/6$. The critical condition shows that the flow is stable, no fingers form until the circle radius grows to a certain radius. This can be called a critical radius ξ_c. In fact, ξ changes with time τ, which means a critical time τ_c. In $0<\tau<\tau_c$, there are no fingers, but fingers arise and grow for $\tau_c<\tau$.

B. Maximum growth rate

From Eq. (24), the time-dependent growth rate is

$$\alpha=\frac{f'(\tau)}{f(\tau)}=-\frac{6P\xi n^3+(m+1)n^2-[6\xi(P+\xi)-m(6\xi^2+1)+1]n+6(m+1)\xi^2}{\xi^2[(m+1)n^2-(m-1)n+6(m+1)\xi^2]}. \tag{29}$$

After extending α to continuous rather than discrete n, we find Eq. (30) from the condition $\partial\alpha/\partial n=0$. Thus

$$3(m+1)P\xi n_{\max}^4-6(m-1)P\xi n_{\max}^3-(m+1)[3(m-1)\xi^2-3P\xi(18\xi^2+1)+(m-1)]n_{\max}^2$$
$$+6\xi^2(m+1)[3(m-1)\xi^2-3P\xi+(m-1)]=0, \tag{30}$$

where $n_{\max}$ is the finger number for which α is maximum and is the only one positive real-valued solution of Eq. (30). Then, the P for $n_{\max}$ is expressed as

$$P=\frac{(m^2-1)(n_{\max}^2-6\xi^2)(3\xi^2+1)}{3n_{\max}^2[m(n_{\max}-1)^2+(n_{\max}+1)^2]\xi+18\xi^3(m+1)(3n_{\max}^2-1)}, \tag{31}$$

and especially for $m=0$, the capillary number N_{Ca} in Eq. (23) will be given as

$$N_{\mathrm{Ca}}=-\frac{n_{\max}^4+2n_{\max}^3+(18\xi^2+1)n_{\max}^2-6\xi^2}{4(n_{\max}^2-6\xi^2)(3\xi^2+1)}. \tag{32}$$

IV. COMPARISON WITH EXPERIMENTS OF MAXWORTHY (REF. 12)

In gas/liquid displacement, we can put $m=0$ with only a very small error. P, rather than N_{Ca}, is constant, as is shown in Eq. (23), when the gas flow rate Q is constant.

In the abstract of Maxworthy[12] on radial injection, he referred that

> "Experiments on the stability of the circular interface formed in a Hele-Shaw cell when air displaces a viscous oil have shown that available theories underestimate the wavelength of the most unstable wave when the capillary number (N_{Ca}) is large. Apparently this is caused by a modification of the interface boundary condition by three-dimensional effects. At small values of N_{Ca} the results overlap several of the theories and we are unable to choose among them on the basis of the present experiments."

Maxworthy[12] discussed the theories of Paterson,[1] Chouke *et al.*,[4] Park and Homsy,[6] and Schwartz.[7] The only calculations for radial fingering are Paterson[1] and now, VPF. The other calculations are for channel flow where the maximum growth rate is determined by maximizing the growth rate over a continuum of wavenumbers defined by perturbations of a flat interface. Channel fingering is rather different than radial fingering because the important time dependence

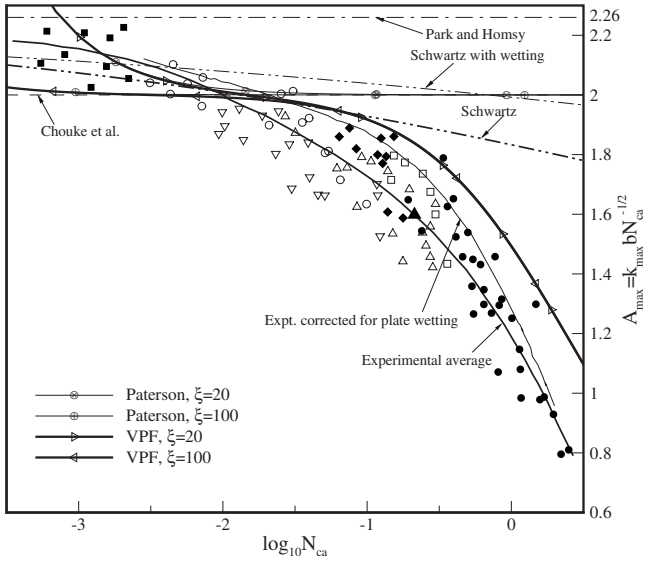

FIG. 1. Modified wave number for the most unstable wave vs capillary number. The experimental points are from Maxworthy (Ref. 12) and for values of b and μ equal to: (○) 0.034 cm, 1.17 P; (▽) 0.065 cm, 1.17 P; (△) 0.128 cm, 1.17 P; (□) 0.191 cm, 1.17 P; (●) 0.0153 cm, 0.061 P; (■) 0.065 cm, 9.95 P; (◆) 0.128 cm, 9.95 P;. The point ▲ corresponds to the case shown in Fig. 3 in Maxworthy (Ref. 12). The calculation of VPF theory, shown as very dark lines is based in Eq. (30) with $R=7.5$ cm and $\xi=R/b$. VPF overestimates the modified wavenumber A_{max} for most data point but is the only theory that represents the trend of results for large N_{Ca} (large b or μ).

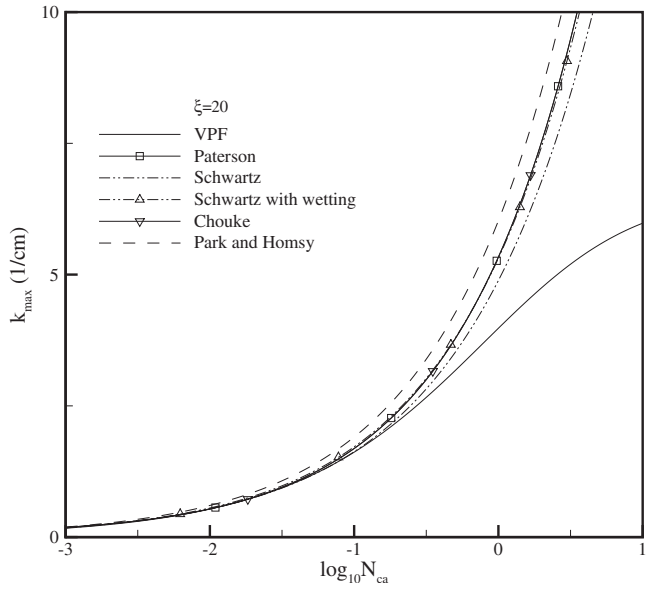

FIG. 2. Maximum wavenumber k_{max} vs capillary number with $\xi=20$. When N_{Ca} is large, the difference between the wavenumber k_{max} for maximum growth between VPF and other theories is large because VPF takes into account the effects of the viscous normal stress.

of the basic flow in Eq. (1) is absent and the action of surface tension in radial fingering is unlike that at plane interface. The comparisons of theories for channel fingering with Maxworthy's[12] experiments are at least one step away from direct. He plotted

$$\log_{10} N_{Ca} \quad \text{vs} \quad A_{max} = bk_{max}/\sqrt{N_{Ca}}, \tag{33}$$

where

$$k_{max} = n_{max}/R \tag{34}$$

and found that $A_{max}=2$ for Chouke *et al.*,[4] 2.26 for Park and Homsy[6] and Schwartz[7] accounted for wetting effects. His results are compared to others and with experiments in Fig. 2 of Maxworthy;[12] he writes

> "An initially circular interface of large diameter, approximately 15 cm, was formed by injecting air very slowly into the central supply hole. the inflow velocity was sufficiently slow that no unstable waves were formed. At the initiation of an experiment the flow rate was suddenly increased to a larger constant value, the interface velocity V increased, a thicker layer of oil was left on the plates, and after a short time instability waves appeared and grew on the interface (Fig. 3). The values of b, μ, and V used were such that at least 30 waves were always formed, so that enough waves were generated to give a good average value for the wave number of maximum growth rate."

The results of our potential flow theory (VPF) are compared to experiments by Maxworthy[12] and theoretical results of other authors in Figs. 1–3. In Fig. 1, the VPF results are computed from Eqs. (33) and (34) for given values of $\xi=R/b$, $R=7.5$ cm, b and N_{Ca} is given by Eq. (32). The inclusion of the viscous normal stress results in a longer wavelength.

Substitute Eqs. (23), (33), and (34) to Eq. (31) with $m=0$, the relation between A_{max}, N_{Ca}, and ξ is expressed as

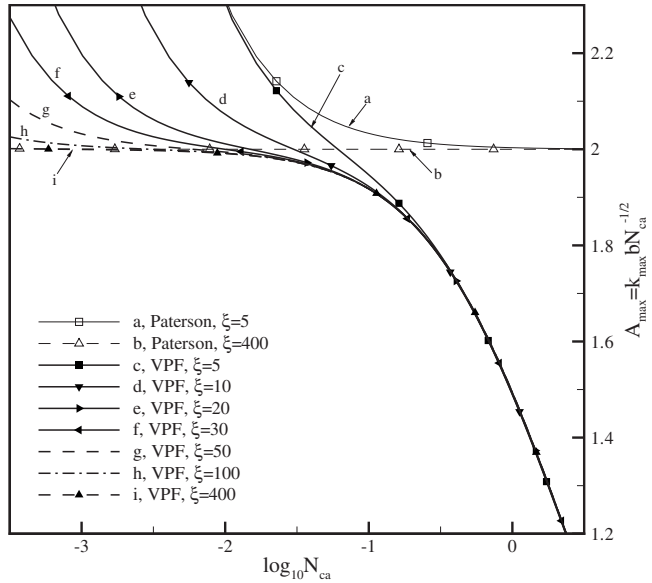

FIG. 3. Comparison of growth rate curves for radial fingering computed from Paterson (Ref. 1) and VPF. For any given value of ξ, A_{max} for VPF lies below A_{max} for Paterson, well below when N_{Ca} is large.

$$3\xi^5 N_{Ca}^2 A_{max}^4 + 6\xi^4 N_{Ca}^{3/2} A_{max}^3 + 3\xi^3 N_{Ca}[4N_{Ca}(3\xi^2+1)+(18\xi^2+1)]A_{max}^2 - 18\xi^3[4N_{Ca}(3\xi^2+1)+1]=0. \quad (35)$$

Using the scaling of order parameter to obtain the relation of A_{max} and high $N_{Ca}(\gg 1)$, the modified wavenumber A_{max} can be established as

$$A_{max} \approx \sqrt{\frac{6}{N_{Ca}}} - \frac{3\xi(2\sqrt{6}\xi+1)}{2N_{Ca}^{3/2}(3\xi^2+1)}. \quad (36)$$

V. EXPLICIT FORMULA FOR THE PERTURBED INTERFACE AND THE CASCADE TO HIGHER-ORDER MODES

In the theory of linear instability of steady flows, we consider disturbance amplitudes proportional to $\exp(\alpha t)$ with growth rate α. For the radial injection problem, the basic flow Eq. (1) depends on time and will not admit exponential growth. The analog of $\exp(\alpha t)$ is $f(t)$ and f'/f is the analog of α.

In linear theories of stability of steady flow, $\exp(\alpha t)$ tends to infinity with time t and α is bounded and it's the same in the radial injection problem. In the unstable case $f(t)\to\infty$ as $t\to\infty$ and f'/f is bounded. Of course, the amplitudes do not grow to the sky before they are saturated by nonlinear effects.

Referring to Eq. (17), we note that $\alpha(t)=f'/f(t)$ can be expressed in terms of R alone where $R(t)$ is related to t by $\pi R^2=\pi R_0^2+Qt$.

We may write

$$\alpha(R(t)) = \frac{1}{f(t)}\frac{df(t)}{dt} = \frac{1}{f(t)}\frac{dR}{dt}\frac{df(t)}{dR} = \frac{1}{f(R)}\frac{Q}{2\pi R}\frac{df(R)}{dR}, \quad (37)$$

and the form of explicit formula is shown in Eq. (38).

$$\int_0^t \alpha(R(t))dt = \int_{R_0}^{R(t)} \alpha(R(t))\frac{dt}{dR}dR = \int_{R_0}^{R(t)} \alpha(R(t))\frac{2\pi R}{Q}dR = \ln[f(R)/f(R_0)]$$
$$= -\frac{2\pi\sigma M_1 M_2(n^3-n)}{bQ\sqrt{(M_1+M_2)[M_2(n^2-n)+M_1(n^2+n)]/6}}\left\{\arctan\left[\frac{\sqrt{6(M_1+M_2)}R}{b\sqrt{M_2(n^2-n)+M_1(n^2+n)}}\right] - \arctan\left[\frac{\sqrt{6(M_1+M_2)}R_0}{b\sqrt{M_2(n^2-n)+M_1(n^2+n)}}\right]\right\} - \frac{M_2(n+1)+M_1(n-1)}{M_2(n-1)+M_1(n+1)}\ln[R/R_0]$$
$$+ \frac{M_1^2(n+2)(n-1)-2M_1M_2n-M_2^2(n-2)(n+1)}{2(M_1+M_2)((n-1)M_2+(n+1)M_1)} \times \ln\left[\frac{6(M_1+M_2)R^2+b^2[M_2(n^2-n)+M_1(n^2+n)]}{6(M_1+M_2)R_0^2+b^2[M_2(n^2-n)+M_1(n^2+n)]}\right]. \quad (38)$$

It follows from Eq. (38) that

$$f(R) = f(R_0)\exp\left[\int_0^t \alpha dt\right] = f(R_0)\exp\left[\frac{2\pi}{Q}\int_{R_0}^{R(t)} \alpha(R(t))RdR\right], \quad (39)$$

where $\alpha=f'/f$ given by Eq. (17) depends on $R(t)$ and n and not explicitly on t or R_0.

Equations (38) and (39) depend on the initial values $R(0)$ and $R(t)$. As $R(t)$ increases, the spectrum of unstable waves increases, more and more fingers nucleate. How may this global property be interpreted?

Let us suppose, as is shown in the experiments of Maxworthy,[12] that at a certain radius, say $R=7.5$ cm, 33 fingers nucleate. The plot of $f(R)$ where $R(0)=7.5$ cm and $R=8.0$ cm is shown in Fig. 4(a). As time goes on, the radius at the tip of the finger increases to a radius where more fingers would nucleate if the radius R were not disturbed. Cardoso and Woods[9] called this a cascade to higher-order modes.

How is this cascade realized when fingers have already nucleated? Obviously we get new fingers on the old fingers [see Fig. 4(b)]. Such a process could be called *tip splitting* with the caveat that at this stage it is probable that nonlinear effects would come into play and the fingers would split at the sides as well as tips. This kind of dynamics could lead to the fractal-like structures seen in fingering experiments.

VI. DISCUSSION AND CONCLUSIONS

We found that when the volume flow rate Q is constant, P given by Eq. (23) is constant but the capillary number N_{Ca} depends on $R(t)$. P, rather than N_{Ca}, is the primary parameter for radial fingering.

The discrepancy between previous theories of fingering in radial injection of gas into liquid at large capillary numbers and the experiments of Maxworthy[12] has been removed by analysis using viscous potential flow. This method has

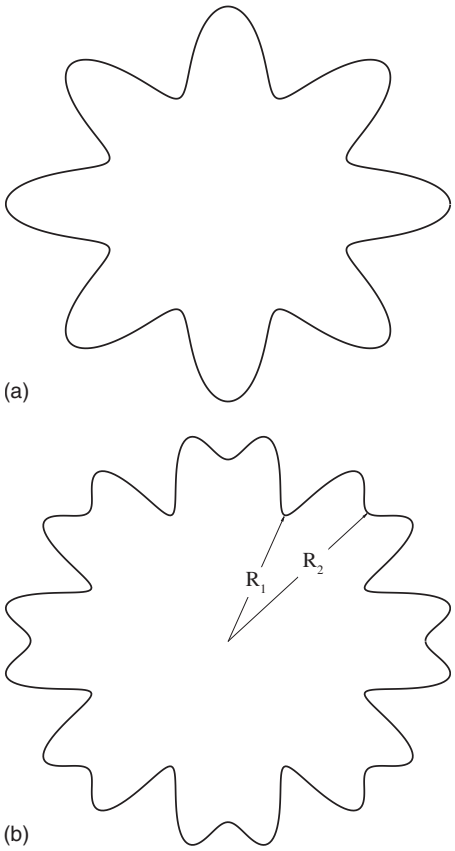

FIG. 4. (a) Finger patterns computed from Eqs. (38) and (39) for $n=8$ for water-air case ($Q=0.01$ m^2/s, $b=0.034$ cm, $R_0=7.5$, and $R=8$ cm). (b) Cartoon of *tip splitting* induced by the linear spreading of unstable waves as R increases. Waves form at $R=R_1$; at $R=R_2$, two new waves nucleate at the tips. Actually the number of waves that would nucleate would be larger than 8 but less than 16. This means that tip splitting due to the nucleation of new waves as R increases would be irregular resembling strongly the configuration of waves shown in Fig. 1 of Paterson (Ref. 1) and Figs. 2 and 3 of Chen (Ref. 13).

been shown to introduce effects of the viscous normal stress at the free surface neglected by all other authors.

The maximum growth rate $\alpha_{\max}$ of VPF can arise at $k_{\max}$, which we could compare as $A_{\max}$ in Fig. 1 with experiment of Maxworthy.[12] The $\alpha_{\max}$ and $k_{\max}$ of VPF are both smaller than those of Paterson[1] which cannot arise for smaller $A_{\max}$ and larger N_{Ca}, being *Hadamard unstable*.

We have conjectured that the cascade to higher-order modes as R increases, as predicted by the linear theory, will lead to repeated splitting of fingers which have already nucleated. The precise description of such splitting dynamics is at present not understood.

Our analysis, like Paterson,[1] is restricted to purely irrotational motions. Though Paterson's flow depends physically on viscosity, the mathematical formulation is precisely that appropriate to the potential flow of an inviscid fluid in which the pressure balances the surface tension as is done in nearly all classical solutions studied by Lamb, Taylor and many other authors. As is true for many of these classical solutions, the addition of an irrotational viscous normal stress brings these classical solutions into a better agreement with experiments and exact analysis.

ACKNOWLEDGMENTS

We wish to thank George Homsy for discussions of fundamental issues generated by viscous displacement. We are grateful to Tony Maxworthy for his help in interpreting the results in his (1989) experiments. This work was supported, in part, by the applied math division of the NSF.

APPENDIX: COMMENTS ON BOUNDARY CONDITIONS AND INSTABILITY MECHANISMS

The authors of Kim *et al.* shared their manuscript with me in advance of its submission to Physics of Fluids, after which the editor invited me to contribute an Appendix. Accordingly, the purpose of this Appendix is to make some general comments about paper, to provide some justification for their use of approximate boundary conditions, and to discuss the physical mechanism of wave number selection.

1. Comments

Viscous fingering in Hele-Shaw cells is often analyzed using depth-averaged quantities, averaged over the thin dimension, b. This results in a set of equations analogous to Darcy's law in which the pressure is a potential for the two-dimensional velocity field, with the coefficients in these equations computed assuming that the flow is a Poiseuille flow in the thin dimension. Two issues then arise: (i) what is the justification for assuming these equations hold at an interface (where the assumption of Poiseuille flow must necessarily break down), and (ii) since the depth-averaged equations are lower order than the (Navier–) Stokes equations, what are the boundary conditions to be applied to solutions of these equations? The resolution of such issues has been the subject of many investigations[6,12,14–18] with the general result that the fields computed from the depth-averaged equations (henceforth referred to as the "outer solutions" of the "outer equations") are subject to corrections within a distance of $O(b)$ of the interface, and that the smooth but rapid variation in pressure can be replaced by a jump condition at the interfacial position, projected onto the bounding plane of the Hele-Shaw cell. These jump conditions are derived in the spirit of matched expansions, where "inner" solutions valid near the interface are matched asymptotically to the outer solutions. Dimensional analysis and scaling indicate that (in addition to the viscosity and density ratios), two parameters govern the problem: an aspect ratio of macroscopic length gap width, ($\xi=R/b$ in the present context), and a capillary number, $\mathrm{Ca}=\mu U/\sigma$. When both Ca and $1/\xi$ are small, they combine to form the "modified capillary number," $\mathrm{Ca}'=\xi^2\,\mathrm{Ca}$, yielding the so-called Hele-Shaw equations.[15] In particular, the pressure jump at the interface, computed from the outer solutions, satisfies

$$[p]=\sigma\cos(\theta)/b+f(\theta)\sigma/R+O(\mathrm{Ca}^{2/3}), \tag{A1}$$

where [ ] notation denotes a jump condition and $f(\theta)$ is a function of the contact angle.[16] [Both $\cos(\theta)$ and $f(\theta)$ are taken, somewhat inconsistently, to be unity by Kim *et al.*] The correction terms have been computed *for wetting fluids* through a Bretherton-type analysis[6,17] for small Ca, and nu-

merically otherwise.[14] There are similar correction terms for the kinematic condition that take into account the small jump in the average velocity due to some of the displaced fluid being left on the walls. Taking only the lowest order terms, linear stability theory predicts that the wavelength of the maximum linear instability growth scales as

$$\lambda \sim b(\mathrm{Ca})^{-1/2}. \tag{A2}$$

These predictions are in disagreement with experiments for large modified capillary number. In particular the experiments of Maxworthy[12] show that for radial injection,

$$\lambda \approx 5b, \quad \mathrm{Ca}' \gg 1, \tag{A3}$$

i.e., the fingering is on the scale of the gap width. This discrepancy is usually attributed to "three-dimensional effects," but attempts to explain it by including correction terms in Eq. (A2) and in the kinematic condition have proven unsuccessful.

The paper by Kim *et al.* advances a totally new approach toward resolving the discrepancy, which is to consider the total normal stress (rather than only the pressure) in formulating jump conditions. They further take the bold step of evaluating the viscous normal stress from the outer solutions for the velocity field. The result is to bring theory and experiment into much better agreement: in particular, they find that the normal viscous stress, as evaluated from the outer solution, is capable of providing a cutoff of small scale instabilities, with the result that for the conditions of Maxworthy's experiments, their Eq. (35) is equivalent to

$$\lambda \sim 2.6b. \tag{A4}$$

This is the only theoretical result providing this level of agreement, which is remarkable and certainly worthy of further discussion, explanation, and justification.

The analysis of Kim *et al.* applies boundary conditions at the interface evaluated using the depth-averaged outer fields, their Eq. (4). All else follows from this equation, which begs two important questions: (i) what are the approximations involved in computing the viscous normal stress from the outer, depth-averaged fields, and can they be justified, and (ii) what is the physical mechanism responsible for the result in Eq. (A4)?

2. Justification of approximate boundary conditions

Justification for the computation of the normal viscous stress at the interface from the outer flow fields requires some thinking about the details of the flow in the thin gap. Two distinct situations may be identified. The first, not of relevance to the experiments of Maxworthy, is when the fluids are partially wetting so that dynamic contact lines are present. The correct computation of the normal viscous stress involves the solution of the Stokes or Navier–Stokes equations, something that to my knowledge has been achieved only for the special case of 90° contact angle in tube flow.[18] What can be stated in general is that the apparent contact angle differs from the static value by a term of $O(\mathrm{Ca})$, leading to a small, $O(\mathrm{Ca})$ correction to Eq. (A1).

The second situation, relevant here, is for wetting fluids such as silicone oils used by Maxworthy in which there is a thin layer of the viscous fluid left on the walls of the Hele-Shaw cell. The thickness of this layer is known to be small for small Ca. The meniscus shape in the thin gap is similarly known to be approximately cylindrical in this limit. Since the meniscus is moving with a steady speed, the instantaneous streamlines in the laboratory frame are horizontal near the centerline while away from it they must bend (i) because of the shape of the meniscus, (ii) in order to accommodate the effect of the wetting layer and (iii) in order to adjust to a Poiseuille profile far from the interface. The effective permeability relating the velocity to the pressure will vary with axial position, reflecting the variation with distance from the nose of the shape of the velocity profile in the thin dimension. Since this affects only constants of proportionality between the pressure and velocity, the *depth-averaged* normal viscous traction vector $2\mu e_{ij}n_j$, where e_{ij} is the rate of strain tensor, is given correctly *in order of magnitude* by the potential flow.

The computation by Kim *et al.* of the normal viscous stress as *if it were acting on a vertical interface* is clearly an additional approximation: a more refined calculation will not alter the basic physical mechanisms and scalings discussed in more detail in the next section, but it will change the numerical coefficients. It remains an open question as to whether accounting for the bending of the streamlines and the resolution of the normal stress along the direction of propagation of the interface will improve the numerical agreement between Eqs. (A3) and (A4).

3. Mechanism

The question naturally arises as to how the viscous normal stress is responsible for stabilization of short waves leading to the result, Eq. (A4), in the absence of the usual stabilization due to the capillary pressure produced by the transverse curvature. Of course the answer is embodied in Eqs. (28) and (29) but in an opaque way. A simple approximate analysis in the limit of large azimuthal wave number, n, small but fixed b, large viscosity contrast, and negligible surface tension gives considerable insight.

Since the bulk dynamics are quasistatic, the kinematic condition, Eq. (12), governs the time dependence of small perturbations. Using the expression for ϕ_{01}, it is easy to show that the first two terms of Eq. (12) [taking a time scaling for which $Q/(2\pi)=1$ for simplicity], give

$$da/dt = -a/R^2. \tag{A5}$$

Equation (A5) is equivalent to the author's Eq. (19) and indicates that for unit viscosity ratio, the interface is stable. Therefore the expression for the perturbation normal velocity $-(\phi_{1j})_r$ is at the heart of the issue as it gives the potential for instability. This quantity is determined by the normal stress balance, Eq. (14).

It is easy to show that the viscous normal stress of the base state is insignificant in influencing the growth rate. A simple calculation shows that the first bracketed term in Eq. (14),

$$[(p_0 + 2\mu\phi_{0,rr})_r]_{r=R} = (\mu_2 - \mu_1)(12/(b^2R) + 4/R^3). \quad \text{(A6)}$$

Since $\xi=(R/b)\gg 1$, the contribution of the normal viscous stress to the destabilizing terms is negligible and the destabilizing term is *identical to that which obtains in the absence of the viscous normal stress*, i.e.,

$$[(p_0 + 2\mu\phi_{0,rr})_r] \approx 12(\mu_2 - \mu_1)/(b^2R). \quad \text{(A7)}$$

The influence of the viscous normal stress therefore arises primarily from the dynamics of the perturbations. The full numerical results of Kim *et al.* show that when surface tension is negligible the instability is characterized by a very large azimuthal wave number, n. Inserting the expressions for the potentials for the perturbation flow, Eq. (11), into the normal stress balance, and taking the limits $n\gg 1$, b fixed, $\sigma=0$, and $\mu_2\gg\mu_1$ (appropriate to the experiments) one finds that the normal viscous stress exerted by the more viscous fluid dominates the pressure of the perturbation flow due to the higher order of differentiation with respect to r. In this limit, the normal stress balance requires that the *viscous normal stress balances the destabilizing term*, Eq. (A7), with the result that

$$\phi_{1r} = -6a/(b^2n^2). \quad \text{(A8)}$$

Then, the dynamic equation becomes

$$da/dt = a/R^2\{-1 + 6R^2(b^2n^2)\}, \quad n \gg 1, \quad b \quad \text{fixed}. \quad \text{(A9)}$$

The second (destabilizing) term arises from the balance of the destabilizing pressure gradient in the base flow with the normal viscous stress of the perturbation flow. The result, Eq. (A9) is incapable of making predictions of the wave number of maximum growth rate, as it is asymptotic for very large n, but it is easy to see that the cutoff value of n is $O(R/b)\gg 1$, with the result that

$$\lambda \sim b. \quad \text{(A10)}$$

[1] L. Paterson, "Radial fingering in a Hele-Shaw cell," J. Fluid Mech. **113**, 513 (1981).
[2] S. Hill, "Channeling in packed columns," Chem. Eng. Sci. **1**, 247 (1952).
[3] P. G. Saffman and G. I. Taylor, "The penetration of a fluid into a porous medium or Hele-Shaw cell containing a more viscous liquid," Proc. R. Soc. London, Ser. A **245**, 312 (1958).
[4] R. L. Chouke, P. van Meurs, and C. van der Poel, "The instability of slow, immiscible, viscous liquid-liquid displacements in permeable media," Trans. AIME **216**, 188 (1959).
[5] S. D. R. Wilson, "A note of the measurement of dynamic contact angles," J. Colloid Interface Sci. **51**, 532 (1975).
[6] C.-W. Park and G. M. Homsy, "Two-phase displacement in Hele-Shaw cells: Theory," J. Fluid Mech. **139**, 291 (1984).
[7] L. Schwartz, "Stability of Hele-Shaw flows: The wetting-layer effect," Phys. Fluids **29**, 3086 (1986).
[8] D. A. Reinelt, "The effect of thin film variations and transverse curvature on the shape of fingers in a Hele-Shaw cell," Phys. Fluids **30**, 2617 (1987).
[9] S. S. S. Cardoso and A. W. Woods, "The formation of drops through viscous instability," J. Fluid Mech. **289**, 351 (1995).
[10] L. M. Martyushev and A. I. Birzina, "Specific features of the loss of stability during radial displacement of fluid in the Hele-Shaw cell," J. Phys.: Condens. Matter **20**, 045201 (2008).
[11] E. Pitts, "Penetration of fluid into a Hele-Shaw cell: The Saffman–Taylor experiment," J. Fluid Mech. **97**, 53 (1980).
[12] T. Maxworthy, "Experimental study of interface instability in a Hele-Shaw cell," Phys. Rev. A **39**, 5863 (1989).
[13] J.-D. Chen, "Growth of radial viscous fingers in a Hele-Shaw cell," J. Fluid Mech. **201**, 223 (1989).
[14] D. A. Reinelt, "Interface conditions for two-phase displacement in Hele-Shaw cells," J. Fluid Mech. **183**, 219 (1987).
[15] G. M. Homsy, "Viscous fingering in porous media," Annu. Rev. Fluid Mech. **19**, 271 (1987).
[16] C.-W. Park, Ph.D. thesis, Stanford University, 1985.
[17] F. P. Bretherton, "The motion of long bubbles in tubes," J. Fluid Mech. **10**, 166 (1961).
[18] F. Kafka and E. B. Dussan V., "On the interpretation of dynamic contact angles in capillaries," J. Fluid Mech. **95**, 539 (1979).